Hydrogen Firing in a Tangentially Fired Boiler Burner

Presented at
American Flame Research Committee Combustion Symposium
Hilton Garden Inn Calgary Downtown, Calgary, Alberta Canada
September, 2024

By
Kevin Anderson, William Barrett, Virginia Garrison, Steve Londerville, and Matthew Whelan
John Zink Company, LLC

Abstract

Design considerations for the conversion of tangentially fired boilers burners from traditional fossil fuels to hydrogen are presented. Operational differences observed with hydrogen combustion compared to combustion of traditional fossil fuels (such as widened flammability limits; increased flame speed; and lack of soot, CO, and VOC potential) are generally viewed as favorable. However, these differences can lead to significant design challenges when converting existing combustion equipment that was originally designed and optimized for fossil fuel operation. The engineering efforts applied to address these design challenges including analytical evaluation of hydrogen combustion for the specific design conditions and scale burner testing are presented.

Introduction

Tangentially-Fire Boilers

Tangentially-Fired (or Corner-Fired) boilers were initially developed for the combustion of solid fuels such as coal and liquid fuels such as heavy fuel oil. Tangentially-Fired Boilers are fitted with burner fuel and air injection columns at the corners of the furnace that deliver fuel and air in a swirling pattern relative to the furnace centerline. Singer described in [1] that this method of introduction of fuel and air into the furnace resulted in the furnace acting as the burner flame mixer with less intense heat transfer on the radiant tube surfaces, and more uniform heat distribution within the furnace. Further, the furnace residence time is very high compared to other types of furnaces and mixing of the air and fuel injections at the corners is in part caused by the furnace swirl pattern. This unique arrangement results in both simplistic and complicated design requirements that are critical to resolve.

Figure 1 shows the predicted flame profile in a four-level tangentially-fired boiler with tilting burners. The image, generated from results from a Computational Fluid Dynamics (CFD) study, show the swirling combustion pattern quite clearly.

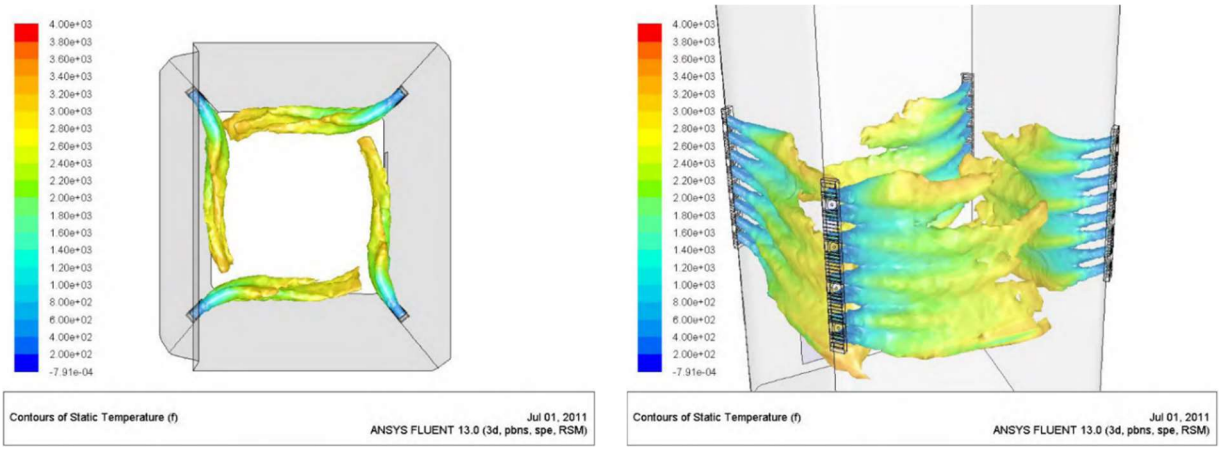

Figure 1 – Predicted Flame Pattern in a Four-Level Tangentially-Fired Boiler

Many Tangentially-Fired boilers exist in industry today, with capacities ranging from approximately 100 million Btu/hour to over 6 billion Btu/hour. Burners for tangentially-fired boilers are generally divided into stabilizer, fuel, and auxiliary air compartments. Airflow to each compartment is generally separately controlled by individual windbox dampers. Smaller capacity units may be fitted with single elevation burners with a single compartment. Larger capacity units would likely be fitted with multi-level burners with multiple fuel and auxiliary air compartments.

Smaller industrial boilers may have non-tilting burners. However, in larger boilers it is common for the individual burner compartments to be designed such that they can be tilted upwards or downwards during firing. Generally, the burner nozzle tilts more downward as firing rate and steaming rate increase. By operating the boiler in this fashion, it is possible to control heat transfer and furnace exit gas temperature in the radiant section, which is crucial to controlling steam temperature in the superheater.

The design of tilting burner compartments often includes a central swirler, center oil gun, and two (2) gas compartments above and below the swirler. Due to the tilting requirement of the compartment, fuel gas injectors are typically recessed.

Figure 2 depicts a portion of a tilting tangentially-fired burner column. In the figure, compartments for one elevation are labeled. Note that burner in the image was illuminated by flame produced by a side - wall igniter. Proving flame attachment and main furnace "fire ball" can be challenging due to the corner arrangement utilizing tilting bucket compartments and reduced air flow in the near field fuel injection zone. Further refractory throats or quarls are not utilized. Historical conversions of these boilers from liquid and solids fuels to gaseous fuels can result in unwanted pulsations and require unique injector designs to enhance local stability.

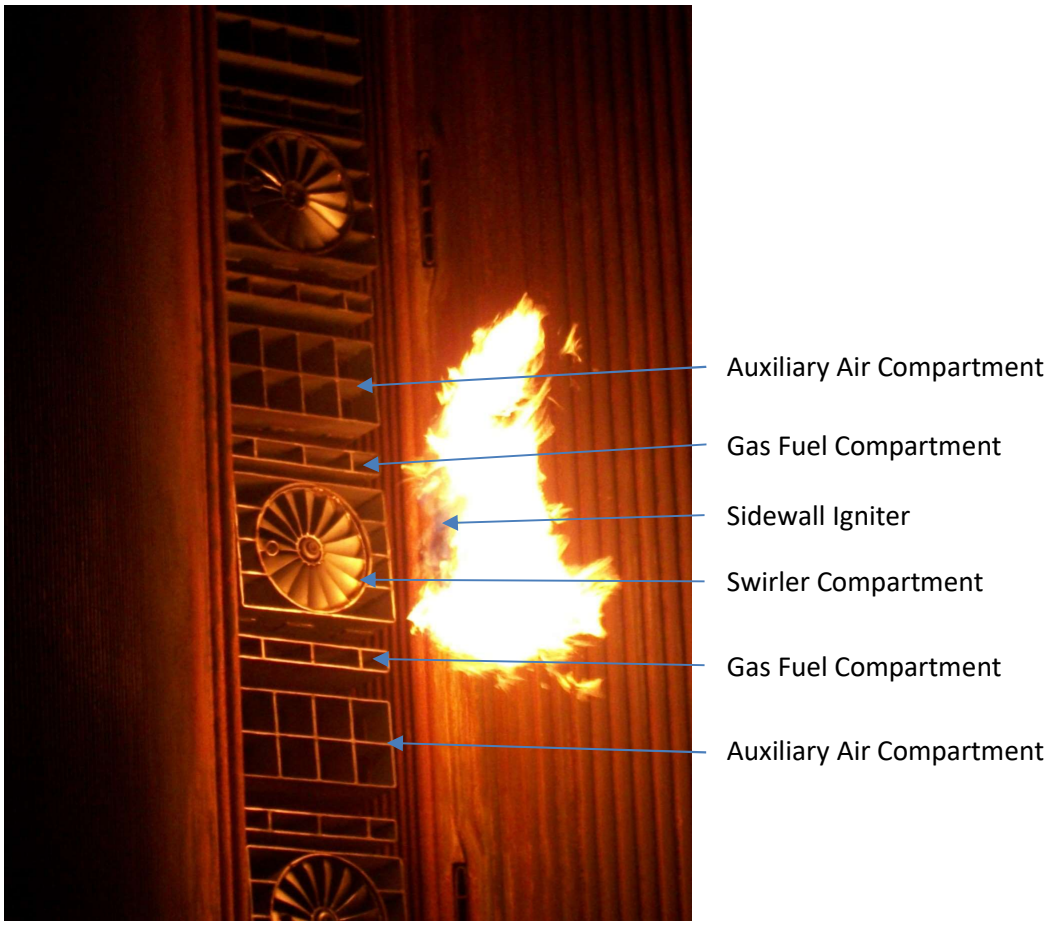

Figure 2 - Tangentially Fired Burner with One Elevation Labeled

Conversion from Natural Gas Firing to H2 Firing

There are many design challenges and opportunities when transitioning from firing conventional fuels to H2 firing. A succinct description of many pros and cons of H2 as a fuel was presented by Baukal et al in [2]. From a design perspective, the detailed flame properties from initial injection to furnace exit need to be modeled in some form for a successful conversion that is in part, presented next.

Londerville and McElroy presented specific challenges for conversion from heavy fuel oil firing to natural gas firing in tangentially-fired boilers in [3]. Key combustion related design challenges presented were assessing the impact to the boiler heat transfer and assessing the pollutant emissions. Those challenges also exist when converting fuel from natural gas firing to H2 firing. Another important combustion related design challenge posed by H2 firing is the thermal design of the combustion equipment.

Flame Speed

It is necessary to compare flame speeds for the fuel-air mixtures considered. Laminar flame speed was predicted for CH4-Air mixtures at 80°F and 650°F for various equivalence ratios using Cantera [4] with the GRI-Mech 3.0 [5] reaction mechanism and is shown in Figure 3. Similarly, laminar flame speed was predicted for H2-Air mixtures at 80°F and 650°F for various equivalence ratios using Cantera [4] with the UCSD [6] reaction mechanism and is also shown in Figure 3

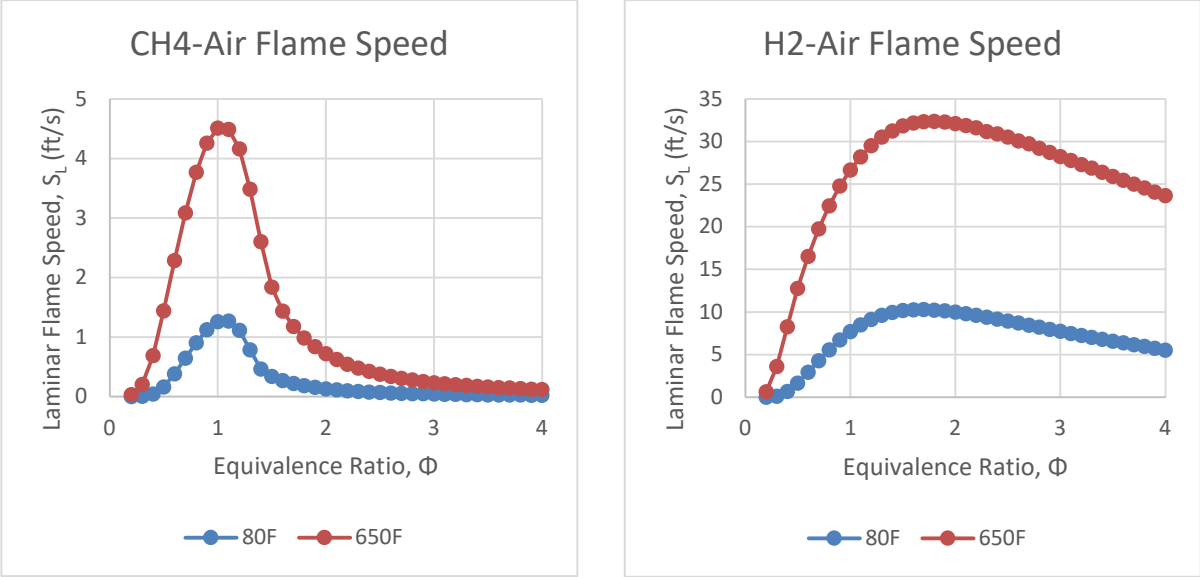

Figure 3 – Laminar Flame Speed for CH4-Air and H2-Air Mixtures

The flow regimes of interest in the tangentially fired burner and furnace are complex and certainly turbulent. Still, comparing laminar flame speeds provides qualitative understanding of the challenges faced in terms of thermal design. Peak flame speed for the H2-Air mixture increased by approximately 3 times when mixture temperature was increased from 80°F and 650°F. Peak flame speed for the H2-Air mixture at 650°F was approximately 7 times faster than the peak flame speed for the CH4-Air mixture at the same temperature. One would expect that the flame front would much more readily propagate upstream for the 650°F H2-Air mixture compared to the CH4-Air mixture at the same temperature.

Limits of Flammability

Kuchta compiled and shared flammability characteristics of CH4 and other hydrocarbons with varying temperatures, pressures, and atmospheres in [7]. The upper and lower limits of flammability (ULF and LLF, respectively) for CH4-Air mixtures at 1.0 atmosphere pressure were extracted from [7] and are shown in Figure 4.

Similarly, Shroeder and Holtappels compiled and shared flammability characteristics of H2-Air and H2-O2 mixtures at various temperatures and pressures in [8]. The upper and lower limits of flammability (ULF and LLF, respectively) for H2-Air mixtures at 1.0 atmosphere pressure were extracted from [8] and are shown in Figure 4.

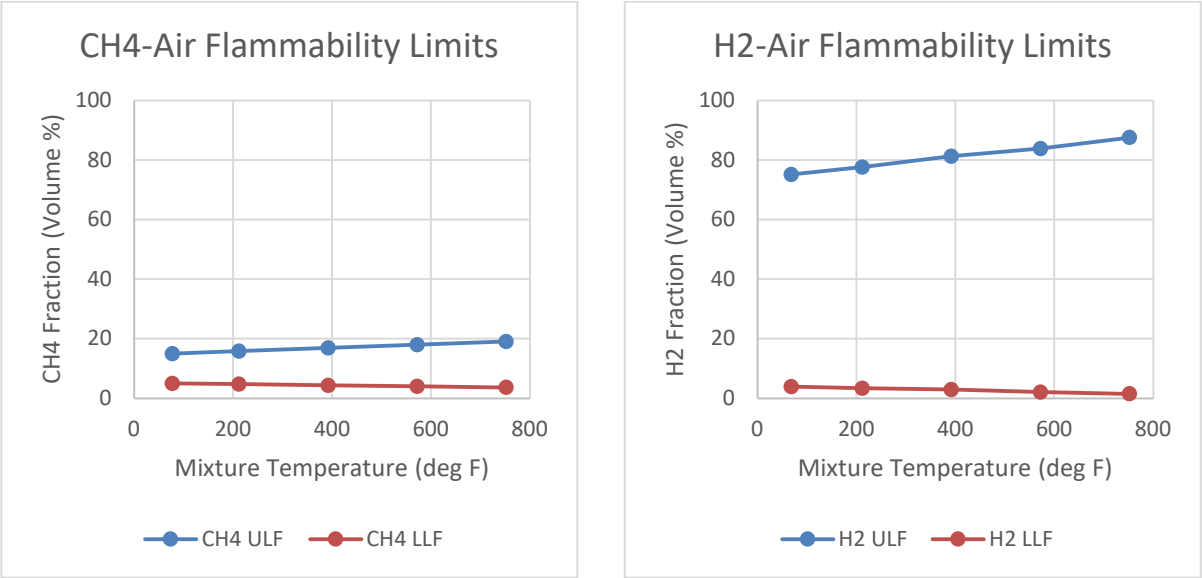

Figure 4 – Flammability Limits of Fuel-Air Mixtures

Jet Entrainment (Concentration vs diameter downstream)

A typical tangentially-fired burner fuel injector is recessed within the metal burner grid. The fuel jets emitted from the fuel injector will entrain combustion air as the jets flow through the burner grid and into the furnace. As a first step, it is useful to compare the rates of entrainment for CH4 jets vs H2 jets. Beér and Chigier suggested in [9] that the following correlation be used to estimate the rate of entrainment for a free jet:

$$\frac{\dot{m}_a}{\dot{m}_0} = 0.32 \left(\frac{\rho_a}{\rho_0}\right)^{1/2} \frac{x}{d_0} \qquad \textit{Eq. 1}$$

Where:

$\dot{m}_a$	=	Mass flow of entrained air.
$\dot{m}_0$	=	Mass flow emitted from fuel nozzle.
ρ_a	=	Density of the entrained air.
ρ_0	=	Density of the fuel emitted from the nozzle.
x	=	Distance from nozzle exit.
d_0	=	Jet diameter at nozzle exit.

In [9], Beér and Chigier also suggest the following useful normalized correlations to estimate the velocity and concentration of fuel within a fully developed jet as:

$$\frac{\bar{u}_0}{\bar{u}_m} = 0.16 \frac{x}{d_0} \left(\frac{\rho_a}{\rho_0}\right)^{1/2} - 1.5 \qquad \textit{Eq. 2}$$

$$\frac{\bar{u}}{\bar{u}_m} = exp\left[-K_u \left(\frac{r}{x}\right)^2\right] \qquad \textit{Eq. 3}$$

$$\frac{C_0}{C_m} = 0.22 \frac{x}{d_0} \left(\frac{\rho_a}{\rho_0}\right)^{1/2} - 1.5 \qquad \textit{Eq. 4}$$

$$\frac{C}{C_m} = exp\left[-K_c \left(\frac{r}{x}\right)^2\right] \qquad \textit{Eq. 5}$$

Where:

$\bar{u}$	=	Axial velocity anywhere in the jet.
$\bar{u}_0$	=	Axial velocity at the nozzle exit.
$\bar{u}_m$	=	Axial velocity on the jet axis.
K_u	=	Empirical constant (with suggested values between 82 and 92).
C	=	Fuel concentration anywhere in the jet.
C_0	=	Fuel concentration at the nozzle exit.
C_m	=	Fuel concentration on the jet axis.
K_C	=	Empirical constant (with suggested values between 54 and 57).
r	=	radial distance from jet axis.

Equation 1 suggests that entrained mass (of air into the fuel jet, in this case) increases linearly with distance from the fuel nozzle exit. Similarly, equations 2 and 4 suggest that jet velocity and jet fuel concentration, respectively, decrease linearly with distance from the fuel nozzle exit. Finally, equations 3 and 5 suggest that jet velocity and jet fuel concentration follow a Gaussian distribution radially with peak values of axial velocity and fuel concentration occurring at the jet centerline as the entrained fluid mixes with the fluid from the jet.

It is interesting to combine the flammability limits shown in Figure 4 with the flow field predicted by equations 2 through 5. By doing so, the predicted flammable regions within the CH4 and H2 jets could be computed and compared. Analysis required integration of the Gaussian functions and was handled numerically using methods outlined in [10]. Ultimately, the fraction of fuel that was predicted to be flammable was computed for each fuel for various downstream distances. These results are shown in Figure 5.

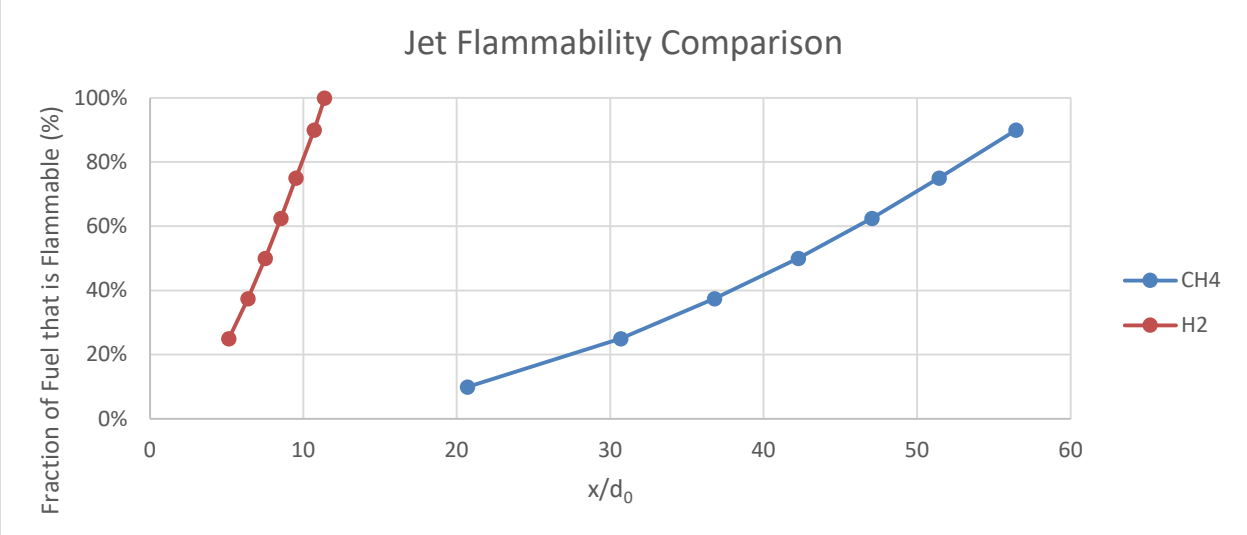

Figure 5 – Jet Flammability Comparison

This analysis was simplified in many ways. For example, the computations ignored the combustion reactions which would certainly increase temperatures and widen the flammability limits. Still, the analysis was useful in that it revealed that a generally similar flammability profile would be realized within the H2 fuel jet in (approximately) 1/5 to 1/6 the distance from the nozzle as compared to the CH4 fuel jet.

NOx Emissions

Of primary interest was the impact on stack NOx emissions due to the transition from natural gas to H2 firing. A succinct description of sources and means to predict NOx emissions from industrial flames was presented by Anderson and Londerville in [11]. For natural gas and H2 combustion with 650°F combustion air temperature, it was concluded that thermal NOx would dominate the NOx emissions.

Thermal NOx emissions can be described using the extended Zeldovich mechanism. The significant reactions are as follows:

$$O + N_2 \rightleftharpoons N + NO \qquad \textit{Eq. 6}$$

$$N + O_2 \rightleftharpoons O + NO \qquad \textit{Eq. 7}$$

$$N + OH \rightleftharpoons H + NO \qquad \textit{Eq. 8}$$

Some simplifications can be made to the thermal NOx calculation. First, Equation 8 is significant only for fuel rich combustion. Thus, Equation 8 can be neglected for lean combustion applications. Second, the quasi-steady assumption for [N] can be used which allows for equations 6 and 7 to be combined since Equation 6 is the limiting step. Finally, reverse reactions can be neglected for tangentially-fired applications since resultant NO concentrations are generally very low compared to equilibrium and the reverse rate is low.

Suitable kinetic rate constants such as those proposed by Bowman [12] or by Baulch et al [13] for Equation 6 can then be applied. In previous work, the authors found that the kinetic rates and simplified chemistry proposed by Monat in [14] to be suitable for tangentially-fired applications utilizing relevant mixing models as:

$$d[NO]/dt = 2K_1[N_2][O]\frac{gmol}{cm^3\ sec} \qquad \textit{Eq. 9}$$

Where:

K_1 = $1.84 \times 10^{14} e^{-E/RT}\ \frac{cm^3}{gmol\ sec}$
E = $76{,}250\ \frac{cal}{gmol}$
R = $1.986\ \frac{cal}{gmol\ K}$
T = Temperature in Kelvin

For tangentially-fired applications, the [O] concentration in Equation 9 can be set to equilibrium concentrations and can be computed based on predicted [O_2] concentration and predicted temperature. Equilibrium [O] can be approximated using the correlation proposed by Westenberg [15] or by interpolation of JANAF thermochemical tables which are available from NIST [16]. The author's preference is to use the Westenberg approximation:

$$[O] = K_0(R\#T)^{-1/2}[O_2]^{1/2}\ \frac{gmol}{cm^3} \qquad \textit{Eq. 10}$$

Where:

K_0 = $3.6 \times 10^3 e^{-3\ ,090/T}(atm)^{1/2}$
$R\#$ = $82.057\ \frac{cm^3\ atm}{gmol\ K}$
T = Temperature in Kelvin

Equations 9 and 10 were combined to arrive at a rate equation that can be used for evaluation of thermal NOx in tangentially-fired units after computation of the oxygen and temperature field as:

$$d[NO]/dt = 1.46 \times 10^{17} T^{-1/2} e^{-69{,}483/T} [N_2][O_2]^{1/2} \frac{gmol}{cm^3\ sec} \qquad \textit{Eq. 11}$$

Using this approach, Equation 11 was then post-processed over the flow field for various fuel cases as outlined by Anderson and Londerville in [11]. The thermal NOx emissions were estimated for natural gas, CH4, and H2 flames using dissociated adiabatic flame temperature with 650°F combustion air temperature and normalized relative to natural gas. The other global variables ($[N_2]$, $[O_2]$, and time) were assumed to be constant for these calculations. This is shown in Figure 6.

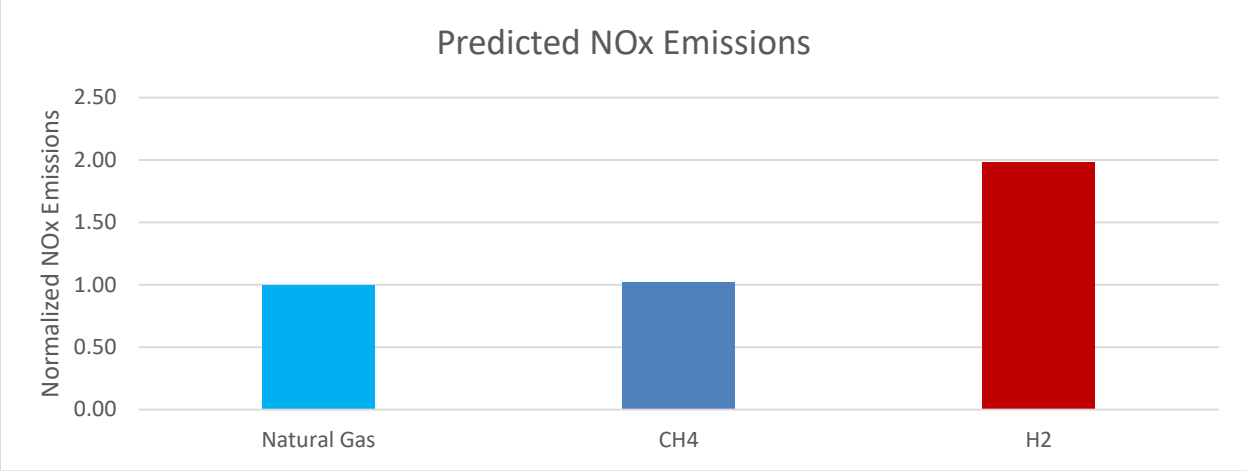

Figure 6 - Predicted NOx emissions for Natural Gas, CH4, and H2 Flames

Heat Transfer

Evaluation of heat transfer is an important aspect of fuel conversions for tangentially-fire boilers. While boiler tubes within the radiant and convection sections are tolerant to changes in heat flux, tangentially-fired boilers very commonly contain pendant superheater banks sensitive to changes in heat transfer. Superheater banks often operate close to the maximum steel and alloy material temperature limits. Often de-superheat water is added to the inlet steam flow to control peak metal and final steam temperatures.

For any fuel conversions of tangentially-fired boilers it is highly recommended that a boiler impact study is executed. These studies use furnace modeling tools to evaluate radiant heat transfer and predict furnace exit temperature at the superheater bank. Studies often recommend mechanical and operating changes to offset changes in heat transfer. These can include changes in burner tilt position, addition of de-superheat flows, or material changes to the superheat bank. While a boiler impact study should be executed on specific projects, some general trends emerge when analyzing the heat transfer impact of hydrogen.

General Radiation and Furnace Exit Temperature Predictions

There are several methods available to predict furnace exit temperature and radiant heat transfer. For a generalized tangentially-fired boiler case with equivalent heat input, stoichiometry, and tilt position, it is expected that the furnace exit temperature will increase by approximately 50-200°F when converting from natural gas to hydrogen. This prediction is a result of both computational fluid dynamic (CFD) methods and computations using correlations such as proposed by Long in [17].

While hydrogen has a higher adiabatic flame temperature compared to natural gas, the flame has a lower emissivity. Emissivity is a function of CO2 and H2O concentrations within the flame body as well as black-body radiation from soot. Since hydrogen contains no carbon, hydrogen flames do not emit soot black-body radiation. This offset is more pronounced with tangentially-fired burners since the emissivity from soot with hydrocarbon flames increases with rich combustion, and tangentially-fired burners often contain high levels of fuel and air staging. Additionally, the total flue gas mass flow rate is 20% lower with hydrogen compared to natural gas due to lower stoichiometric air ratio. The result is less total radiant heat transfer and higher furnace exit temperature. Changes to burner tilt, de-superheat flow, or superheat material may be required for hydrogen conversions.

Procedure

Tangentially-Fired Burner Test

As part of an engineering study, one elevation of a tangentially-fired burner was designed, built, and installed in the test facility in Tulsa, Oklahoma. Following commercial inquiries regarding the applicability of H2 retrofit into existing tangentially-fired boilers, additional testing and subsequent modifications were implemented into this test burner.

The test burner was designed for a nominal firing capacity of 52.6 million Btu/hr LHV maximum heat release rate when firing natural gas. The test burner featured stationary (i.e. non-tilting) burner compartments. The test burner was designed with a simplified upstream air supply configuration without the standard modulating dampers; instead, the tests were performed with fixed dampers maintaining a constant stoichiometry in the burner compartment. The air compartments above and below the burner compartment were included in the test assembly as shown below in Figure 7.

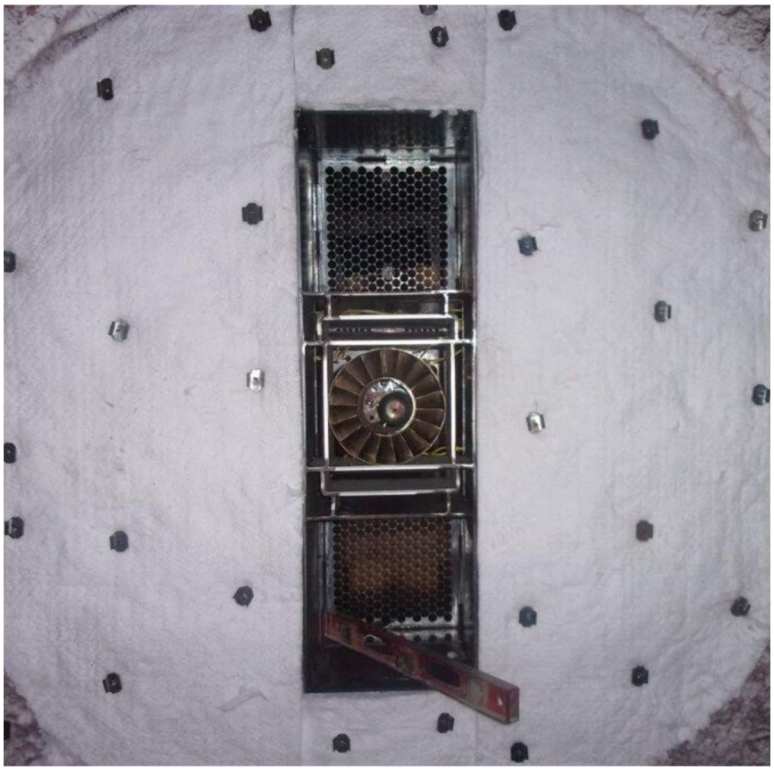

Figure 7 - Overall burner design

Initial testing was performed with natural gas operation. Following commercial interest, H2 compatibility was introduced to the test objectives. The primary goal was to identify the necessary mechanical modifications for robust H2 operation and to evaluate overall burner performance. Given

previous experience with H2 operation, the primary concerns were flame speed and flammability of H2 compared to natural gas. Due to the recessed nozzle design as shown in Figure 8, it was hypothesized that these differences would result in flame stabilization close to the fuel nozzles and would cause localized overheating and excessive warping of the fuel compartment.

Figure 8 – Recessed fuel nozzle layout

To assess this possibility, thermocouples were arrayed around the burner compartment to monitor surface temperatures throughout the operation cycle, as shown in Figure 9. Of particular interest were thermocouple measurements close to the fuel nozzle exit at locations T-17 (inner), T-10 and T-13 (sides), and T-2 (outer).

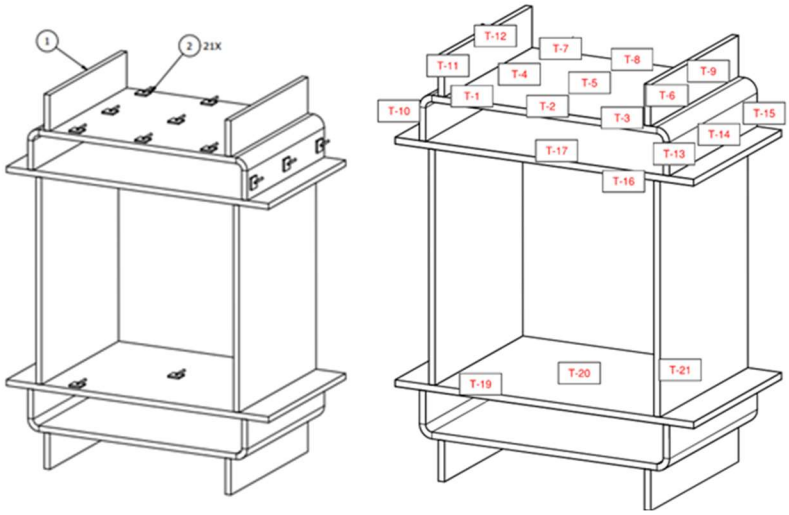

Figure 9 - Thermocouple placement

In total, twenty-one (21) thermocouples were installed on the fuel bucket's surfaces, with insulated wiring to withstand the high air preheat temperatures. Once the fuel bucket was fabricated, the thermocouples were tack-welded to the surface prior to installation, as shown in Figure 10.

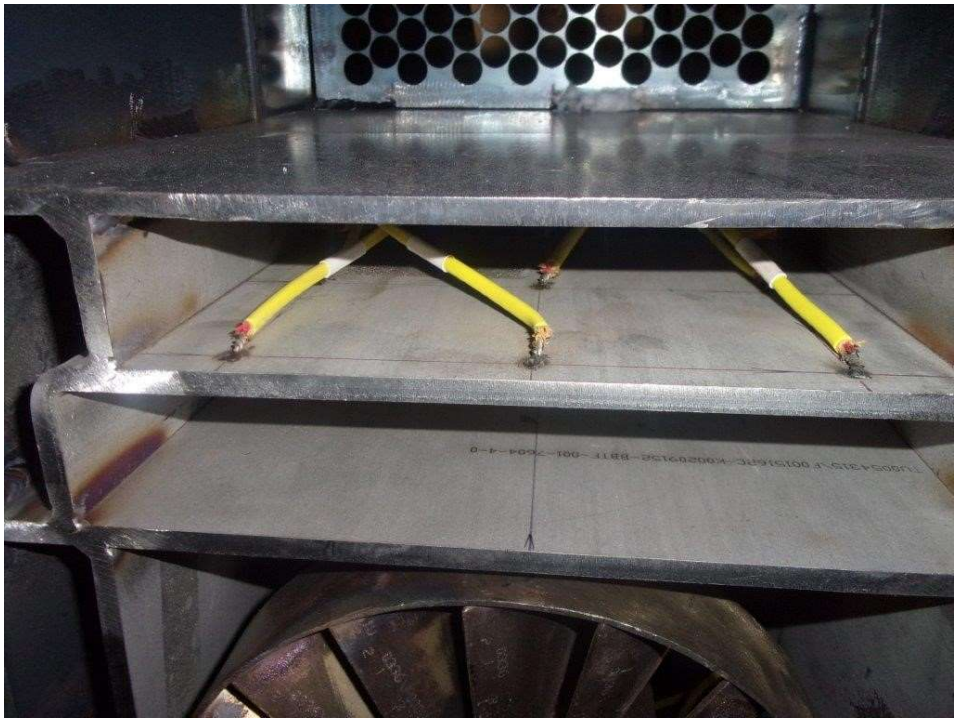

Figure 10 - Tack-welded thermocouple arrangement

Two fuel injector designs were built for the tests. The first design incorporated design features typical for natural gas firing. The second design included enhancements intended to improve performance with H2 firing. The hot ends of the fuel compartments were fabricated from a stainless-steel alloy. Figure 11 shows the installed fuel injectors recessed in the fuel compartments.

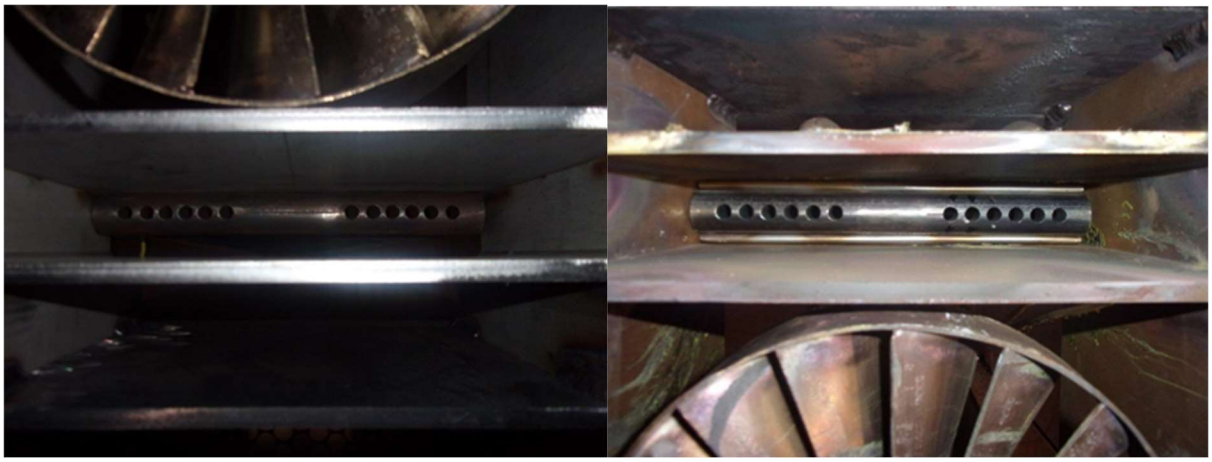

Figure 11 – Fuel Injectors Recessed in Fuel Compartments

F3 Test Conditions

All burner testing was performed in Furnace 3 in the Tulsa Test Center. Furnace 3 is a water-cooled boiler with the internal arrangement as shown in Figure 12.

Figure 12 - Furnace 3 configuration

The natural gas firing and H2 firing tests were conducted with preheated air at 650°F and with 25% global excess air. The firing rate for the natural gas firing and H2 firing tests was approximately 20 million Btu/hr LHV. All testing was performed between December 2023 and April 2024.

Results

Flame Characteristics

Figure 13 depicts the natural gas flame captured from viewports on the side and rear of the furnace. The image shows a normal diffuse blue flame near the fuel nozzle exit and a bushy yellow flame in the furnace downstream.

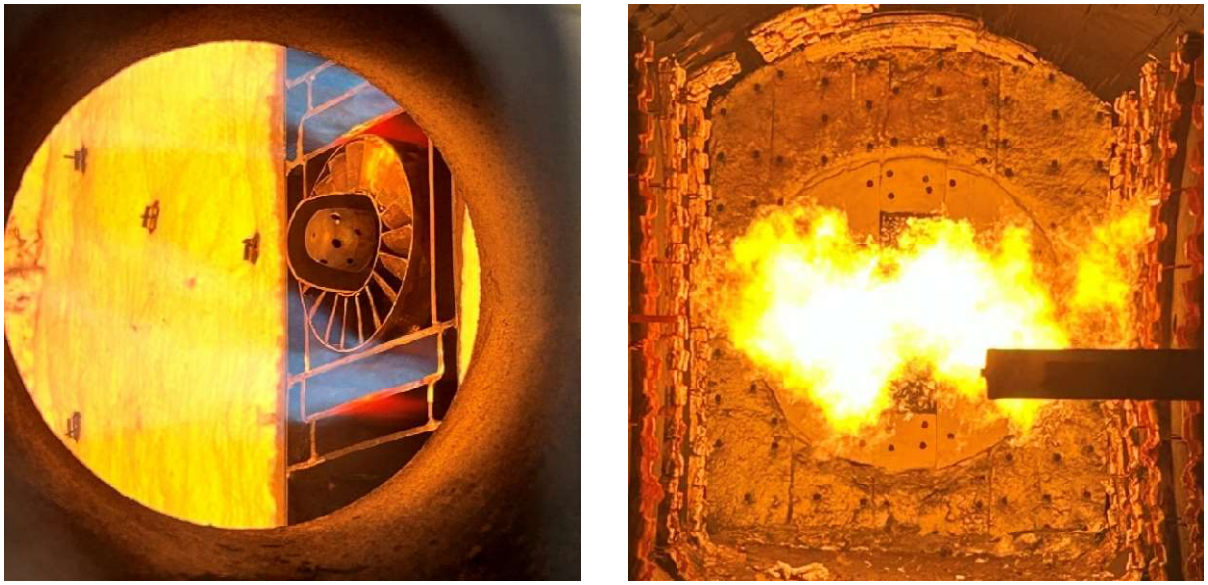

Figure 13 - Natural Gas Flame with Conventional Fuel Drilling

Figure 14 depicts the H2 flame firing from the conventional fuel nozzle captured from the same viewports. The image shows a diffuse flame near the fuel nozzle exit generally similar in appearance to the natural gas flame. The fuel compartment frame can be seen to be glowing much brighter than was evident with the natural gas flame. The view from the furnace exit shows a bushy dusty red flame that is similar in shape to that of the natural gas flame, but much dimmer in appearance.

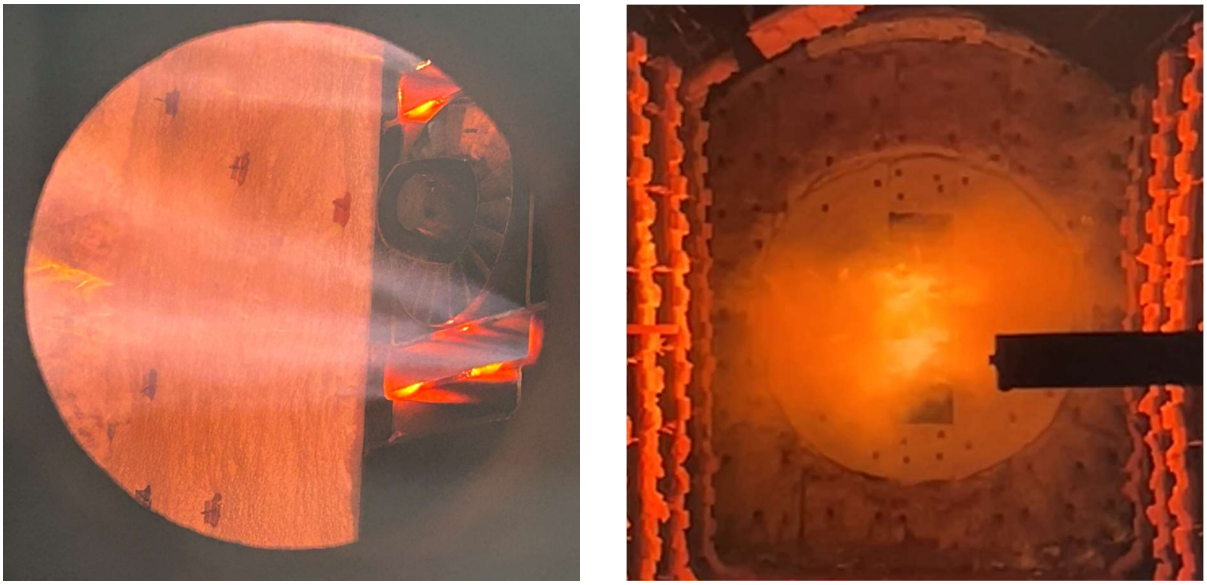

Figure 14 - H2 Flame with Conventional Fuel Nozzle

Figure 15 depicts the H2 flame firing from the modified drilling captured from the same viewports. The image shows a streaky looking flame near the fuel nozzle exit, and the fuel compartment frame is noticeably cooler. The view from the furnace exit again shows a bushy dusty red flame that is somewhat brighter in the center than was observed with the H2 flame with conventional drilling.

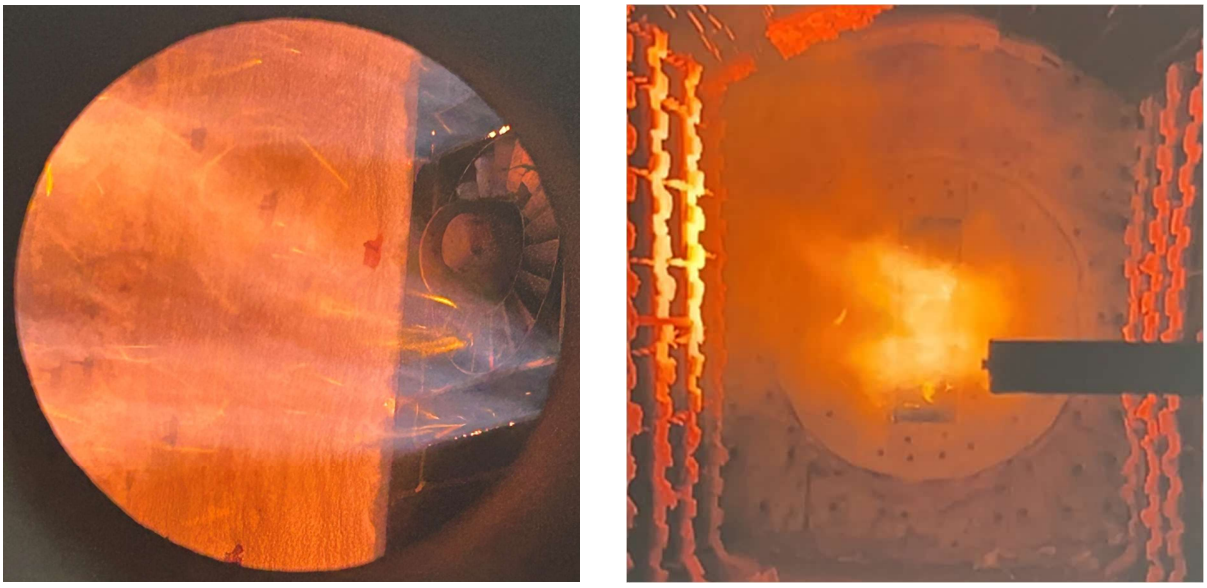

Figure 15 - H2 Flame with Modified Fuel Nozzle

NOx Emissions

Figure 16 depicts the predicted and measured NOx emissions for each of the three cases. The NOx emissions were normalized to the natural gas firing NOx emissions. The NOx emissions measured for H2 firing from the conventional nozzle showed NOx emissions that were approximately 2.6 times the natural gas NOx emissions from the same fuel nozzle. The NOx emissions measured for H2 firing from the modified nozzle showed NOx emissions that were approximately 2.0 times the natural gas NOx emissions from the conventional fuel nozzle.

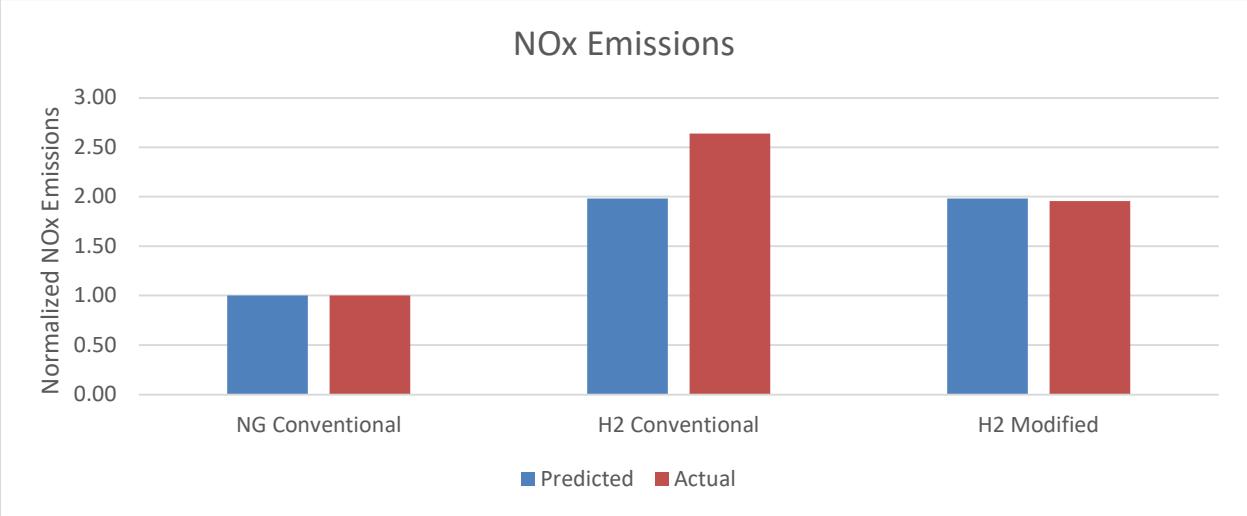

Figure 16 - Measured NOx Emissions for Natural Gas and H2 Flames

Temperature Measurements

Fuel nozzle frame temperature measurements from the fuel nozzle exit at locations T-17 (inner), T-10 and T-13 (sides), and T-2 (outer) are shown in Figure 17 for the natural gas firing case, the H2 firing case with conventional fuel nozzle, and the H2 firing case with the modified fuel nozzle. The absolute temperatures are normalized against the average absolute temperature measured for the natural gas firing case.

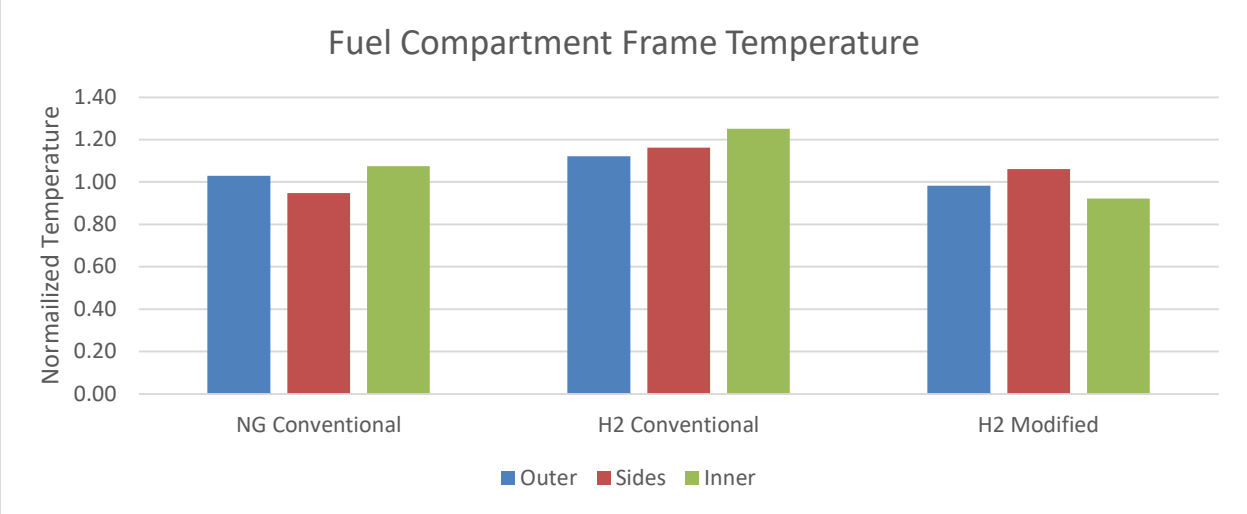

Figure 17 - Fuel Compartment Frame Temperature for Natural Gas and H2 Flames

Discussion and Conclusion

The NOx emissions measured for the H2 firing case with the conventional nozzle were higher than predicted by simply evaluating dissociated adiabatic flame temperature. The fuel nozzle frame temperatures were higher for this case as well. This was due to the H2 flame igniting and combusting significantly faster than was observed with the natural gas flame.

This observation was not surprising. The analysis showed significant increase in laminar flame speed and significantly widened flammability for the H2 fuel compared to CH4. Combining analysis of the fuel flammability limits with analysis of the entrainment and mixing of the H2 and CH4 fuel jets showed a significant increase in flammability near the fuel nozzle. Specifically, it was predicted that a H2 fuel jet would become similarly flammable to a CH4 fuel jet just in 1/5 to 1/6 the distance from the fuel nozzle.

The NOx emissions measured for the H2 firing case with the modified nozzle were much closer to what would be expected by comparing the dissociated adiabatic flame temperature of the H2 flame to that of the natural gas flame. The fuel nozzle frame temperatures, on average, were significantly reduced for this case as well. Clearly, the modifications made to the fuel nozzle were effective in mitigating the effects of the increased flammability characteristics of the H2 fuel.

It was interesting and useful to analyze and address the deleterious factors encountered when firing H2 in a burner system that was more suited for conventional fuels. Through the analysis and testing, remedies for mitigating NOx emissions and burner over-heating were identified and demonstrated using a modified burner that included an enhanced fuel nozzle design along with upgraded burner materials. These solutions are practical, and they are currently being offered to customers.

References

[1] J. G. Singer, Combustion Fossil Power - A Reference Book on Fuel Burning and Steam Generation, 4th Edition, Windsor: Combustion Engineering, Inc., 1991.

[2] M. W. S. L. M. H. G. T. B. J. Charles Baukal, "Hydrogen: Fuel of the Future?," in *ASME International Mechanical Engineering Congress and Exposition*, Virtual, 2021.

[3] S. L. a. M. McElroy, "Conversion of Tangential Fired Utility Furnaces from Oil to Gas," in *American Flame Research Committee Annual Meeting*, Salt Lake City, 2012.

[4] G. H. K. M. I. S. R. L. S. a. B. W. W. David G, "Cantera: An object-oriented software toolkit for chemical kinetics, thermodynamics, and transport processes.," Version 3.0.0 doi:10.5281/zenodo.8137090, 2023. [Online]. Available: https://www.cantera.org.

[5] D. M. G. M. F. N. W. M. B. E. M. G. C. T. B. R. K. H. S. S. W. C. G. J. V. V. L. a. Z. Q. Gregory P. Smith, "GRI-Mech 3.0," [Online]. Available: http://www.me.berkeley.edu/gri_mech/.

[6] "Chemical-Kinetic Mechanisms for Combustion Applications," San Diego Mechanism web page, Mechanical and Aerospace Engineering (Combustion Research), University of California at San Diego, [Online]. Available: http://combustion.ucsd.edu.

[7] J. M. Kutchta, Investigation of Fire and Explosion Accidents in the Chemical, Mining, and Fuel-Related Industries - Bulletin 680, Washington DC: United States Bureau of Mines, 1985.

[8] V. S. a. K. Holtappels, "Explosion Characteristics of Hydrogen-Air and Hydrogen-Oxygen Mixtures at Elevated Pressures," in *International Conference on Hydrogen Safety*, Pisa, 2005.

[9] J. M. B. a. N. A. Chigier, Combustion Aerodynamics, Malabar: Robert E. Krieger Publishing Company, 1983.

[10] A. W. A.-K. a. J. R. Tooley, Numerical Methods in Engineering Practice, New York: CBS College Publishing, 1986.

[11] S. B. L. Kevin M. Anderson, "Practical Use of Computational Fluid Dynamics to Industrial Combustion Applications," in *American Flame Research Committee Combustion Symposium*, Kauai, 2013.

[12] C. T. Bowman, "Kinetics of Pollution Formation and Destruction in Combustion," *Progress in Energy and Combustion Science,* vol. 1, pp. 33-45, 1975.

[13] D. L. Baulch, C. J. Cobos, R. A. Cox, P. Frank, G. Hayman, T. Just, J. A. Kerr, T. Murrells, M. J. Pilling, J. Troe, R. W. Walker and J. Warnatz, "Summary Table of Evaluated Kinetic Data for Combustion Modeling: Supplement 1," *Combustion and Flame,* no. 98, pp. 59-79, 1994.

[14] R. K. H. a. C. H. K. J. P. Monat, "Shock Tube Determination of the Rate Coefficient for the Reaction N2+O2 > NO+N," in *17th Symposium (International) on Combustion*, Pittsburgh, 1978.

[15] A. E. Westenberg, "Turbulence Modeling for CFD," *Combustion Science and Technology,* vol. 4, pp. 59-67, 1971.

[16] NIST, "NIST-JANAF Thermochemical Tables," National Institute of Standards and Technology, September 1982. [Online]. Available: http://kinetics.nist.gov/janaf/html/O-001.html. [Accessed 1 May 2013].

[17] V. D. Long, "Estimation of the Mean Radiating Temperature of a Cylinder of Combustion Gases," *Journal of the Institute of Fuel,* vol. 35, p. 431, 1962.